



UNIVERSITY  
OF WOLLONGONG  
AUSTRALIA

University of Wollongong  
Research Online

---

Faculty of Engineering and Information Sciences -  
Papers: Part B

Faculty of Engineering and Information Sciences

---

2018

# Design, Fabrication, and Test of a Coupled Parametric-Transverse Nonlinearly Broadband Energy Harvester

Thomas Searle  
*University of Wollongong*

Tanju Yildirim  
*Shenzhen University, ty370@uowmail.edu.au*

Mergen H. Ghayesh  
*University of Adelaide, mergen.ghayesh@adelaide.edu.au*

Weihua Li  
*University of Wollongong, weihuali@uow.edu.au*

Gursel Alici  
*University of Wollongong, gursel@uow.edu.au*

---

## Publication Details

Searle, T., Yildirim, T., Ghayesh, M. H., Li, W. & Alici, G. (2018). Design, Fabrication, and Test of a Coupled Parametric-Transverse Nonlinearly Broadband Energy Harvester. *IEEE Transactions on Energy Conversion*, 33 (2), 457-464.

Research Online is the open access institutional repository for the University of Wollongong. For further information contact the UOW Library:  
research-pubs@uow.edu.au

---

# Design, Fabrication, and Test of a Coupled Parametric-Transverse Nonlinearly Broadband Energy Harvester

## **Abstract**

A coupled parametric-transverse nonlinearly broadband energy harvester utilizing mechanical stoppers has been designed, fabricated, experimentally tested, and in some cases theoretically verified. An energy harvester with coupled parametric and transverse cantilever beams with additional tip-masses was excited using an electrodynamic shaker. A piezoelectric bimorph has been attached to each cantilever beam; when the excitation frequency was in the vicinity of the parametric or transverse resonances, the mechanical strain developed in the piezo-bimorphs was converted into electrical energy across a purely resistive ac load. For the cases involving no stoppers, a weak softening-type nonlinear frequency-voltage behavior was observed for the parametrically excited cantilever beam; however, with the addition of mechanical stoppers, both the transverse and parametrically excited cantilever beams displayed a strong hardening-type nonlinear frequency-voltage behavior. The stoppers substantially increased the operating bandwidth for both the parametric and transversely excited cantilever beams compared to the case without stoppers. For the theoretical investigations, a good agreement for both the fundamental frequencies and frequency-response curves was obtained. It is shown that by coupling transverse and parametric cantilevers with mechanical stoppers, the nonlinear energy harvested by the system takes place over a much broader frequency-bandwidth when compared to the singular transverse cantilever mechanism (by about 163.5%).

## **Disciplines**

Engineering | Science and Technology Studies

## **Publication Details**

Searle, T., Yildirim, T., Ghayesh, M. H., Li, W. & Alici, G. (2018). Design, Fabrication, and Test of a Coupled Parametric-Transverse Nonlinearly Broadband Energy Harvester. *IEEE Transactions on Energy Conversion*, 33 (2), 457-464.

# Design, Fabrication, and Test of a Coupled Parametric-Transverse Nonlinearly Broadband Energy Harvester

T. Searle, T. Yildirim, M. H. Ghayesh, Weihua Li, and Gursel Alici

**Abstract**— In this work, a coupled parametric-transverse nonlinearly broadband energy harvester utilising mechanical stoppers has been designed, fabricated, experimentally tested and in some cases theoretically verified. An energy harvester with coupled parametric and transverse cantilever beams with additional tip-masses was excited using an electrodynamic shaker; a piezoelectric bimorph has been attached to each cantilever beam—when the excitation frequency was in the vicinity of the parametric or transverse resonances, the mechanical strain developed in the piezo-bimorphs was converted into electrical energy across a purely resistive AC load. For the cases involving no stoppers, a weak softening-type nonlinear frequency-voltage behaviour was observed for the parametrically excited cantilever beam; however, with the addition of mechanical stoppers, both the transverse and parametrically excited cantilever beams displayed a strong hardening-type nonlinear frequency-voltage behaviour—furthermore, the stoppers substantially increased the

---

T. Searle, T. Yildirim, G. Alici and W. Li are with the School of Mechanical, Materials, and Mechatronics Engineering, University of Wollongong, Wollongong, NSW 2522, Australia.

M. H. Ghayesh is with the School of Mechanical Engineering, University of Adelaide, Adelaide, SA 5005.

operating bandwidth for both the parametric and transversely excited cantilever beams compared to the case without stoppers. For the theoretical investigations, a good agreement for both the fundamental frequencies and frequency-response curves was obtained. It is shown that by coupling transverse and parametric cantilevers with mechanical stoppers, the nonlinear energy harvested by the system takes place over a way broader frequency-bandwidth compared to the case with just a transverse cantilever (by about 163.5%).

**Index Terms**— Energy Harvester; Coupled Motion; Design and test; Nonlinearly Broadband

## INTRODUCTION

IN recent decades, the pursuit of renewable and clean energy technologies has substantially increased due to global energy demands; renewable energy sources include solar, geothermal, and wind [1-5]. Another class of suitable energy technologies are motion based energy harvesters (MBEH); specifically, MBEHs can convert ambient kinetic energy into electricity to power wireless sensor nodes in hostile situations. The energy conversion tools to convert between the mechanical and electrical domains include electromagnetic induction (EMI) [6], electrostatic conversion [7, 8] and using the piezoelectric effect [9].

A major concern for MBEH technology is the effective operating bandwidth at which the core element of the device can harvest energy; both passive and active techniques can be used to achieve an increased operating bandwidth. Frequency-broadening techniques for MBEHs can be grouped into two main categories; these are *linear* and *nonlinear* techniques.

In the first category (i.e. the linear techniques), the literature is extensive. For example, Leland and Wright [10] designed and fabricated an axially compressible tuneable energy harvester; results showed a 24% shift in the fundamental frequency with this design configuration. Yu et al. [11] developed a hybrid linear MBEH with a coupled EMI and piezoelectric generator;

results showed that with a hybrid design the bandwidth of the MBEH slightly increased. Shahruz [12] used a multimodal array of cantilever-beams to increase the effective operating bandwidth of the fabricated MBEH; with slight changes in the tip-mass and beam dimensions, an increased bandwidth was achieved and energy extracted. Challa et al. [13] fabricated a linearly tuneable MBEH using a tuning magnet attached to a cantilever beam; the tuning magnets resulted in a stiffness change of the cantilever beam core element.

For the nonlinear approaches to energy harvesting (i.e. the second category), Leadenham and Erturk [14] developed a hybrid EMI and piezoelectric energy harvester using an M shaped beam as the core element; results showed a hardening-response due to the M shape design. Mann and Simms [15] theoretically and experimentally investigated the energy extraction based on the levitation of same pole magnets; for the theoretical analysis, the method of multiple time scales (MMTS) was used—a comparison between the experimental and theoretical results were shown to be within very good agreement. Daqaq [16] theoretically and experimentally investigated the nonlinear energy that can be extracted from a parametrically excited beam with a piezoelectric bimorph; the MMTS method was employed for the theoretical investigation—results showed a softening-type nonlinear response. Chen and Jiang [17] theoretically investigated an energy harvester with coupled internal resonances using the MMTS; results showed a dual softening and hardening frequency-response could be achieved with this design. Another nonlinear approach for increasing a MBEHs bandwidth is the use of mechanical stoppers; Wu et al. [18] fabricated transversely excited MBEHs using mechanical stoppers to further enhance the operating bandwidth of MBEHs, however, with reduced energy extraction.

In this work, a nonlinearly broadband energy harvester has been designed based on the coupled transverse-parametric motion of two cantilever-beams with mechanical stoppers; a device has been fabricated and experimentally tested; theoretical comparisons were also conducted for some cases, showing very good agreement. Piezoelectric layers were chosen as the transduction mechanism between the mechanical strain

developed in the cantilever-beams and the electrical energy charged by the piezo-bimorph; furthermore, by coupling transverse and parametric motions in conjunction with mechanical stoppers, the fabricated energy harvester has a significantly larger bandwidth compared to the case with one transverse cantilever with no stoppers (by about 163.5%); i.e., the designed system harvests energy from a broad range of ambient vibrations compared to conventional energy harvesters.

### Device design and fabrication

In this section, a detailed description of the energy harvester based on transverse-parametric motions is presented; a theoretical background has also been presented for the main design considerations.

### System Design

Figure 1 shows a schematic of the fabricated energy harvester consisting of a transversely excited cantilever-beam ( $T_b$ ) and a parametrically excited cantilever-beam ( $P_b$ ) which are clamped and connected through an L-shape frame; the piezoelectric bimorph for both the cantilever-beams has been connected to a purely resistive AC load (see Figure 1 (b)). Both the transversely and parametrically excited beams are made of an aluminium alloy and share common mechanical properties with Young's modulus ( $E$ ) of 69.5 GPa, density ( $\rho$ ) of 2700 kg/m<sup>3</sup>, and Poisson's ration ( $\nu$ ) of 0.33. The parametric cantilever-beam of length ( $P_L$ ), width ( $P_B$ ), and thickness ( $P_h$ ) has dimensions 160 mm, 15.85 mm and 0.6 mm, respectively; similarly, the transversely excited cantilever-beam has length ( $T_L$ ), width ( $T_B$ ), and thickness ( $T_h$ ) with dimensions of 180 mm, 15.85 mm and 0.6 mm, respectively. An additional tip mass has been attached to the free end of each cantilever-beam to increase the displacement of the free end and reduce the parametric threshold; for the parametrically excited cantilever-beam ( $P_b$ ), a tip mass of 0.0196 kg ( $m_p$ ) was used—similarly, a tip mass of 0.004 kg ( $m_T$ ) was used for the transversely excited cantilever-beam. For the conversion process between the mechanical strain developed in the cantilever beams and the electrical energy harvested, an MFC M-2807-P1 piezoelectric transducer has been bonded to each beam, 48 mm from the clamped end of the transversely excited beam and 52 mm from the

clamped end on the parametrically excited beam. Each transducer has length ( $L_p$ ) 27.5 mm, width ( $B_p$ ) 9.7 mm and a thickness ( $h_p$ ) of 0.35 mm, respectively. The piezoelectric bimorphs were connected to a purely resistive load of 993 kilo-Ohms for the transversely excited beam and 995 kilo-Ohms for the parametrically excited beam. The frame has been axially excited in a coherent direction to the secondary beam, by a periodic acceleration of  $A\sin(2\pi\Omega t)$ , where  $A$  is the base acceleration amplitude ( $\text{m/s}^2$ ),  $\Omega$  is the excitation frequency (Hz) and  $t$  is time in seconds. To further increase the operating bandwidth of the system, mechanical stoppers have been introduced for each cantilever-beam. Stoppers impact with the beam at certain displacement ranges which results in changing the effective length and stiffness of the beam, hence introducing further nonlinearities that broaden the energy extraction of the fabricated device. The terms  $x_1$  and  $x_2$ ,  $y_1$  and  $y_2$  correspond to the axial and transverse distance of the mechanical stopper tips from the clamped end of the transverse beam, respectively;

similarly,  $x_3$  and  $x_4$ ,  $y_3$  and  $y_4$  represent the axial and

transverse distances of the stoppers on the parametric beam (see Figure 1 (a)).

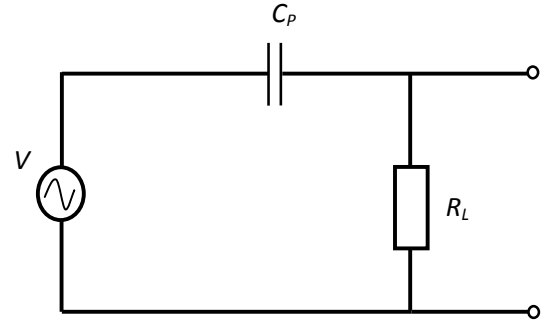
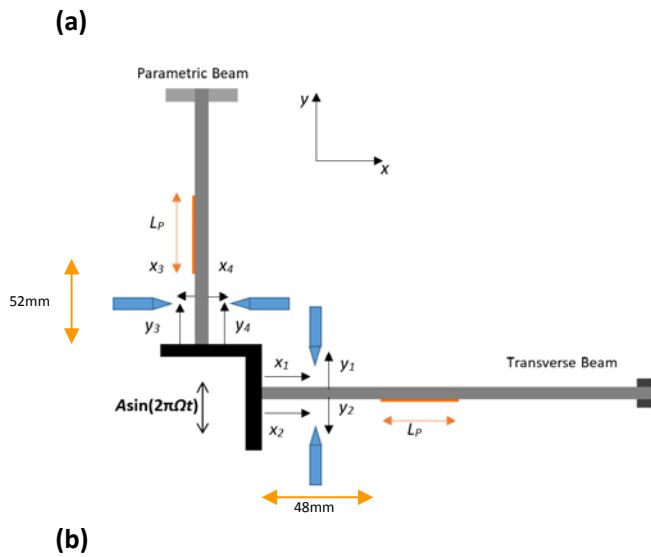


Figure 1: Schematic representations: (a) 2-D schematic of the fabricated coupled parametric-transverse energy harvester; (b) purely resistive AC load.

Table 1: Dimensions of the Parametric and Transverse beams

	Parametric [mm]	Transverse [mm]
Length	160	180
Width	15.85	15.85
Thickness	0.6	0.6
Distance from clamped end to piezoelectric transducer	52	48

Table 2: Material properties of the aluminium alloy used in the system design

	Young's modulus ( $E$ )	Density ( $\rho$ )	Poisson's ration ( $\nu$ )
Aluminium Allot	69.5 GPa	2700 $\text{kg/m}^3$	0.33

### Theoretical background

Typically, for a transversely excited nonlinear system, the governing equation of motion can be modelled using the Duffing equation given by

$$\ddot{x} + \gamma x^3 + \omega x = f \cos(\Omega t), \quad (1)$$

where  $x$  is the displacement field,  $\omega$  is the natural frequency of the system and  $\gamma$  is the nonlinear coefficient. For a parametrically excited system these are theoretically described by

$$\gamma x^3 + [\omega - 2f \cos(2\Omega t)]x = 0, \quad (2)$$

where  $x$  is the displacement field,  $\omega$  is the natural frequency,  $f$  is the forcing amplitude,  $\gamma$  is the nonlinear stiffness term,  $\Omega$  is the excitation frequency and  $t$  is the time.

Parametric systems exhibit large deformations at resonance and when coupled with strain based piezoelectric transducers, produce large voltages at relatively low forcing amplitudes (<1 g). By coupling geometric nonlinearities that arise from large-amplitude motions with coupled excitation directions allows for larger bandwidth at which energy can be harvested; furthermore, the addition of mechanical stopper are also used to further enhance the operating bandwidth of the fabricated energy harvester.

The effective voltage produced by a piezoelectric transducer, when examined in a single strain direction only, can be treated as a parallel plate capacitor as

$$V_c = \frac{d_{31} E_c b_c}{C_p} \int_{l_c} \varepsilon_1 dx, \quad (3)$$

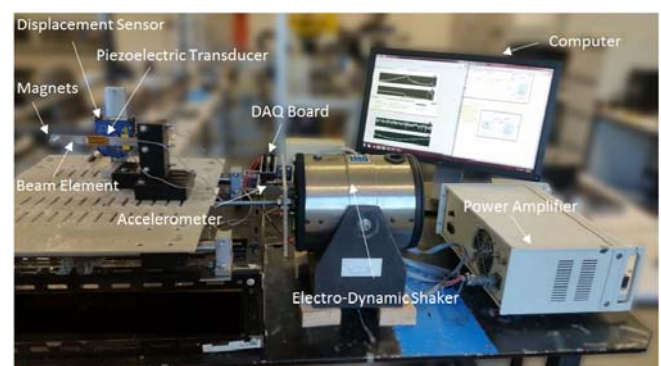
where  $C_p$  is the capacitance,  $l_c$ ,  $b_c$  and  $t_c$  are length, width, and thickness of the transducer, respectively;  $E_c$  is the Young's modulus of the piezoelectric material;  $\varepsilon_1$  is the strain in the axial direction,  $d_{31}$  is the piezoelectric coefficient (C/N or m/V). In the case of the MFC M-2807-P1 transducers, internal capacitance was measured to be 745.9 pF for the transverse beam, and 863.3 pF for the parametric beam (measured at 100Hz).

#### Experimental procedure and measurement setup

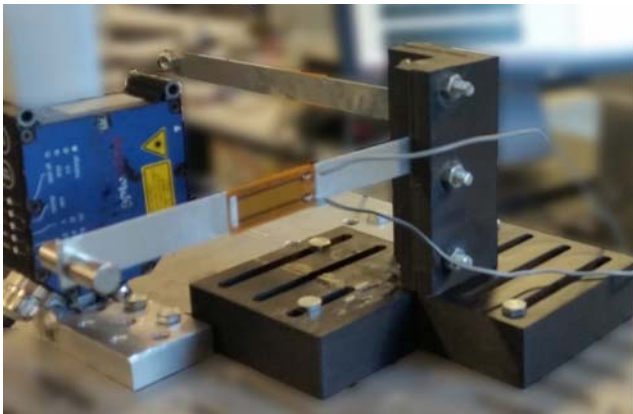
This section describes the experimental procedure used to obtain the frequency-voltage curves of the fabricated energy harvester; detailed explanations of the experimental setup including the instrumentation for measurement are also discussed.

Photographs of the overall experimental setup, close-up of the energy harvester, stoppers on the transversely excited beam and stoppers on the parametrically excited beam are shown in Figures 2 (a) – (d), respectively. An electrodynamic shaker (VTS, VC 100-8), where the input voltage has been amplified using a power amplifier (Sinocera YE5871) has been used to excite the coupled energy harvester in both the transverse and axial directions; the signal from the amplifier was proportional to the output of an analogue channel from the data acquisition board (NI cDAQ-9174, AI module 9201 and AO module 9263) connected to a computer—a constant base excitation was applied to the energy harvester via a closed-loop control system, which is a constant acceleration through the feedback from an accelerometer (CLD Y303). The terminals of both piezoelectric bimorphs were connected to purely AC resistive loads; these are connected in parallel with an analogue input channel; as the cantilever beams developed mechanical strain, the generated voltage from the piezoelectric bimorph was measured through the DAQ. The channels were sampled at a rate of 5 kHz to increase the accuracy of the measured results. Principle results for the transverse and parametric resonances were also observed using a laser displacement sensor (Microepsilon opto NCDT1700ILD1700-50) at a sampling rate of 3 kHz. Sufficient settling time has been allowed between steps to ensure a constant acceleration was maintained, and that the analysis of the system was the behaviour in steady state conditions.”

(a)



(b)



(c)



(d)



Figure 2: Photograph of the experimental setup (a) overview of the entire experimental setup; (b) close-up of the fabricated MBEH; (c) two-stopper configuration; (d) one-stopper configuration.

The overall experimental setup was governed using LABVIEW software, which was responsible for outputting the stimulus signal data to the data acquisition board, and reading in the observed response. This software performs the frequency-sweep based on a variable frequency range, excitation amplitude, and frequency step-size; adequate frequency resolution was required when dealing with the geometric larger-amplitude coupled motion of the system

### Experimental Results

In this section, the dual coupled-excitation nonlinearly broadband energy harvester has been excited in the vicinity of the fundamental resonance for the transverse beam and, at *the same time*, near the principal parametric resonance of the parametrically excited beam; since the configuration of the two cantilevers is in a way that they are perpendicular to each other, an

axial excitation for the first is a parametric excitation for the second. The experimentally obtained root mean square (RMS) frequency-voltage curves for various stopper configurations have been obtained and results are discussed in detail.

### Enhanced operating bandwidth using dual mechanical stoppers

Figures 3 (a) and 3 (b) show the frequency-voltage curves of the fabricated energy harvester when excited near the fundamental resonance of the transverse and in the vicinity of the principal parametric resonance of the parametrically excited core element, respectively. For the transverse beam, *without* any stoppers, a linear response was observed, characterised by a symmetric gradual incline followed by a decline (see sub-figure (a)). With the addition of dual stoppers (configuration B<sub>2</sub> in Table 1), far different results was observed; the system had lower voltage output through the normal resonance region, however, it continued to increase until a discontinuous jump occurred at 8.4 Hz and the system response bifurcated to a (near) zero-response—these points theoretically correspond to saddle-node bifurcations and experimentally occur as jump up and down points. For the parametrically excited core element (see Figure 3 (b)), *without* stoppers, the parametric beam displayed a weak softening-type nonlinear response with the frequency-voltage curves leaning towards the left; moreover, discontinuous jump up and down points occurred; these discontinuous points, theoretically, are due to period-doubling and saddle-node bifurcations. When a dual-stopper configuration was implemented, the parametric beam displayed a strong hardening-type nonlinear behaviour; this response was far different compared to the case without stoppers—a 1385.4% frequency-bandwidth increase was observed (see Figure 3 (b)). Furthermore, this nonlinear behaviour was due to geometric nonlinearities resulting from large deformations and highly nonlinear curvature over the oscillations. The effect of dual stoppers had significant impact as it changed the linear response of a transversely excited cantilever into hardening behaviour (sub-figure (a)), and for the case of the parametric

cantilever, from a weak softening-type behaviour to a strong hardening behaviour (sub-figure (b)). In conclusion, the coupled transverse-parametric motion of the two cantilevers (forming the core elements of the energy harvester) in the presence of stoppers (sub-figures (a) and (b) together) enlarges the operating bandwidth of the device by 163.5% compared to the operating frequency-bandwidth of a device with just a transverse cantilever (which is about 2 Hz); this significant increase in the bandwidth is mainly due to the coupled transverse-parametric nonlinear motion of the system in the presence of motion-limiting constraint by means of external mechanical stoppers.

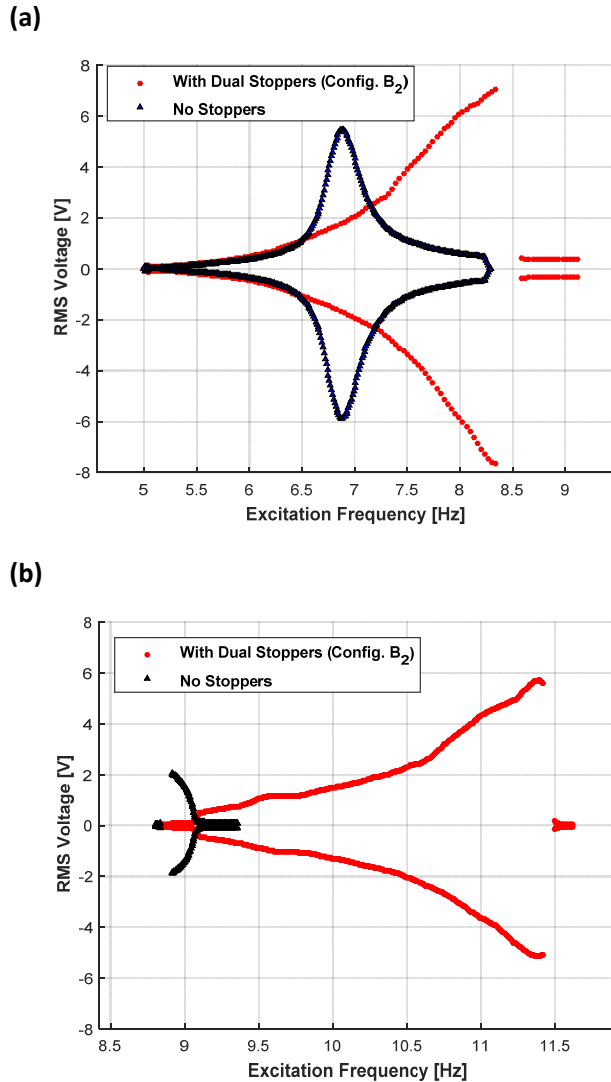
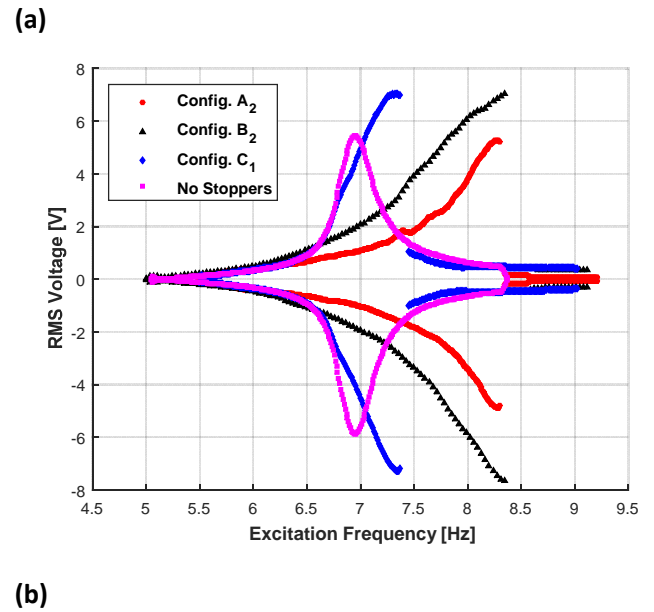


Figure 3: Comparison of the frequency-voltage curves of the fabricated MBEH between no stoppers and dual stoppers: (a) frequency-bandwidth increase due to the transverse cantilever; (b) frequency-bandwidth increase due to the parametric cantilever

Table 3: Stopper configurations used throughout experiments (all dimensions in mm)

Configuration	Transverse Beam				Parametric beam			
	$x_1$	$x_2$	$y_1$	$y_2$	$y_3$	$y_4$	$x_3$	$x_4$
A <sub>1</sub>	48	48	0.28	0.2	48	48	0.28	0.2
A <sub>2</sub>	48	48	0.75	0.83	48	48	0.58	0.75
B <sub>1</sub>	36	36	0.2	0.2	36	36	0.58	0.35
B <sub>2</sub>	36	36	0.75	0.83	36	36	0.58	0.58
C	24	24	0.58	0.58	24	24	0.58	0.58
D	N/A	48	N/A	0.8	48	N/A	1.4	N/A
E	N/A	36	N/A	0.6	36	N/A	0.6	N/A
F	N/A	24	N/A	0.6	24	N/A	0.6	N/A



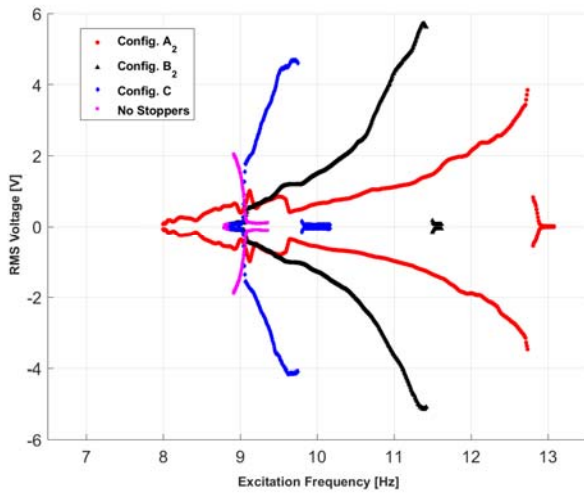


Figure 4: Effect on the frequency-voltage response for fabricated MBEH for different dual-stopper configurations along the length of the cantilever beams (a) for the transverse beam ( $x_1$  and  $x_2$ ) (b) for the parametric beam ( $y_3$  and  $y_4$ ); see Table 1 for the specifications of the different configurations.

The effect of various dual-stopper configurations on the frequency-voltage curves of the transversely and parametrically excited cantilever beams are shown in Figures 4 (a) and (b), respectively. By setting the distance of the stoppers between the clamped-end and the free-end, it was observed the bandwidth and the RMS frequency-voltage curves could be adjusted accordingly. The largest bandwidth was obtained for configuration  $B_2$ , for the case of the transversely excited beam, however, for the case of the parametrically excited beam, it was observed configuration  $A_2$  gave the largest bandwidth of 3.7 Hz. Furthermore, the frequency-voltage curve can be changed with stopper location to either increase power or bandwidth.

A comparison between the lengths and gaps of the dual-stopper configurations for both the transverse beam and the parametric beam are shown in Figures 5 (a) and (b), respectively. It was observed for the transverse beam (see Figure 5 (a)) that with different stopper configurations, a maximum RMS output voltage of 6.5 V was observed, for configuration  $B_2$ , however, the bandwidth of the device was only 0.4 Hz; moreover, configuration  $A_2$  resulted in the greatest bandwidth of 1.85 Hz with a maximum RMS output voltage of 3.9 V. For the case of the parametric beam (see Figure 5 (b)), each frequency-voltage curve displayed a hardening-type nonlinear behaviour. By increasing the gap distance between the stoppers and the beam, it was observed that the frequency-voltage curve had less bandwidth, however, a larger maximum RMS voltage was achieved due to larger axial strains.

(a)

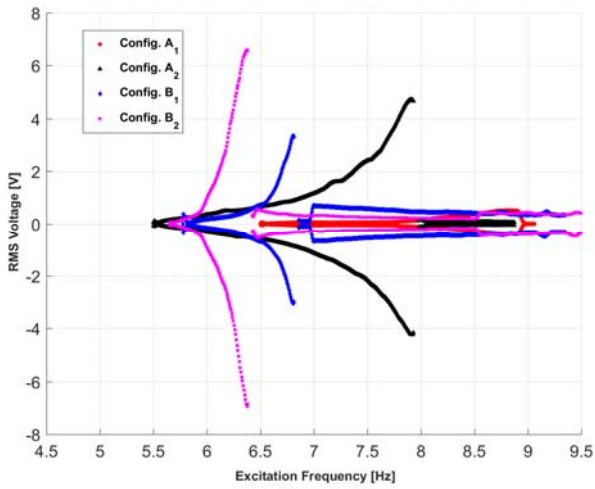


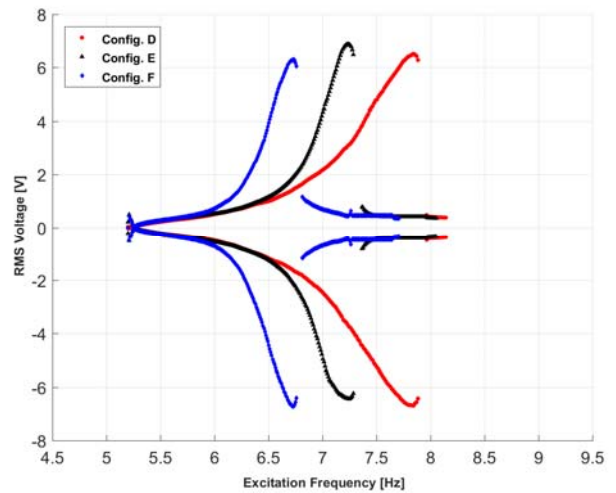
Figure 5: Effect on the frequency-voltage response for fabricated MBEH at different lengths and different gaps from beam. (a) transverse beam ( $y_2$  and  $y_2$ ); (b) parametric beam ( $x_3$  and  $x_4$ )

### Enhanced operating bandwidth using single mechanical stoppers

In this section, the effects of having a single stopper in contact with the transverse and parametric beams have been experimentally investigated and discussed.

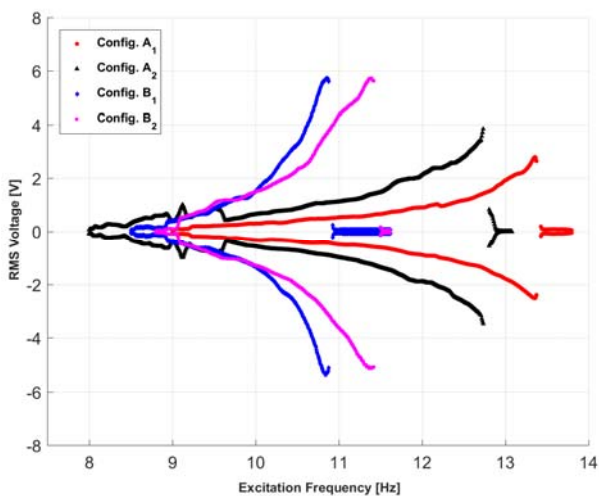
The effects of the single-stopper configuration for the transversely and parametrically beams on the performance of the energy harvester are shown in Figures 6 (a) and (b), respectively. With a one stopper configuration, a strong hardening-type nonlinear behaviour was observed for both the transversely and parametrically excited cantilever beams. Furthermore, configuration D (see Table 1) resulted in the largest bandwidths for both excitations; configuration D also had a maximum RMS voltage of 6.75 V for the transverse beam and 5 V for the parametric beam. In conclusion, when reducing the distance from the clamped-end for both beams a reduction in the bandwidth of the device was observed.

(a)



(b)

(b)



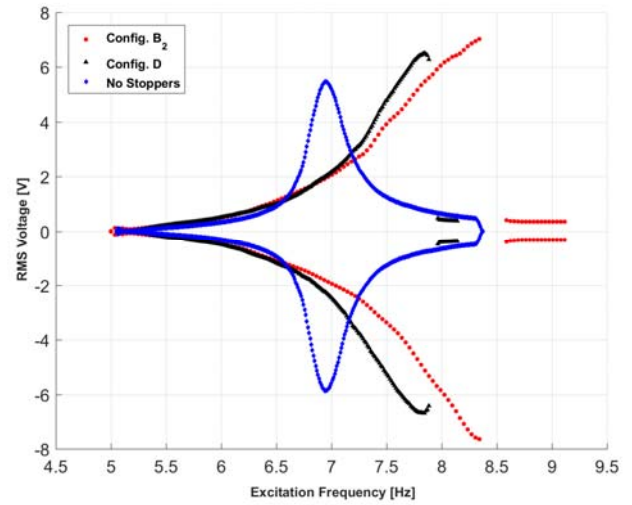
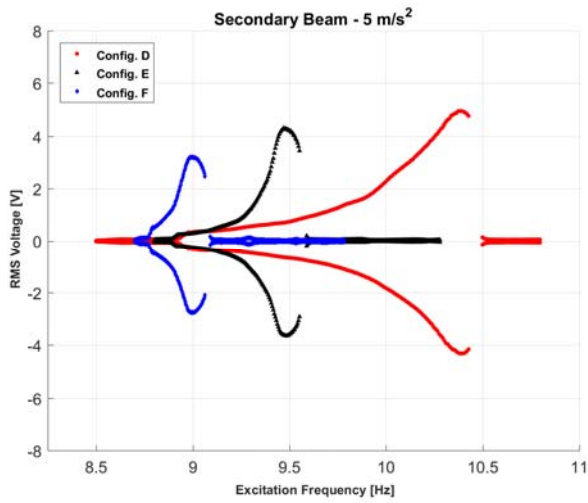


Figure 6: Effect on the frequency-voltage response for fabricated MBEH at different single-stopper configurations along the length of the beam: (a) for the transverse beam ( $x_2$ ); (b) for the parametric beam ( $y_3$ )

### Comparison of different stoppers

A comparison of the optimal dual and single-stopper configurations and no stopper configurations for both the transversely and parametrically excited beams are shown in Figures 7 (a) and (b), respectively. For both the transverse and parametric beams, it was observed, with dual-stoppers configurations the system had larger bandwidth and larger RMS voltage at the maximum response due to energy being extracted at higher frequencies. For the system shown in sub-figure 7 (a) at 7.18 Hz, the corresponding time-trace, close up of the time trace, probability density function and autocorrelation have been plotted in Figure 8, illustrating an asymmetric periodic motion with complexities due to impact between the stoppers and the beams. Furthermore, Table 2 shows a comparison of all the experimentally obtained results for each of the stopper configurations; with dual stoppers a larger bandwidth was achieved.

(b)

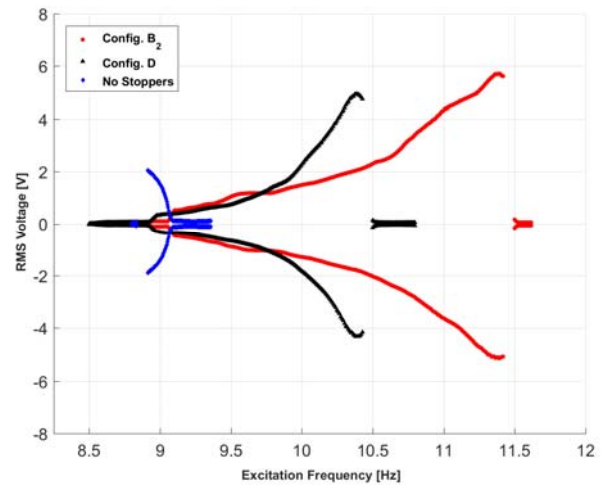
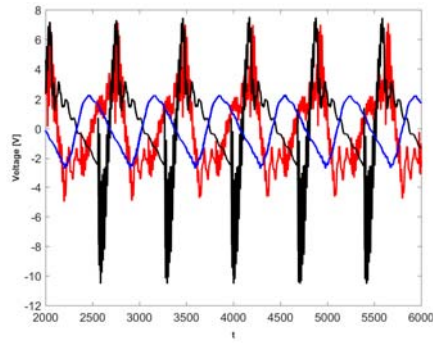


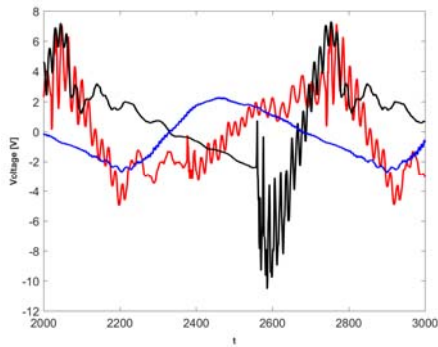
Figure 7: Comparison of the frequency-voltage response of the fabricated MBEH between no stoppers and optimal single and dual-stopper configurations for: (a) transverse beam; (b) parametric beam

(a)

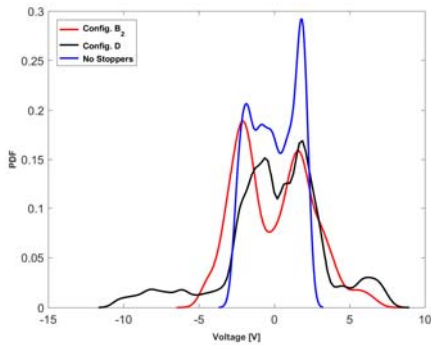
(a)



(b)



(c)



(d)

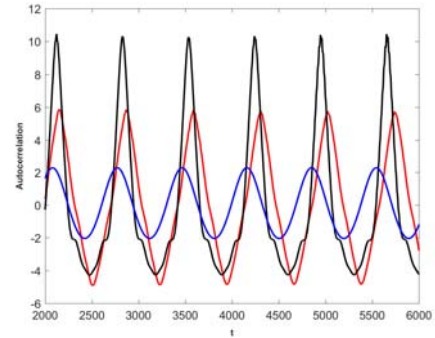


Figure 8: Voltage characteristics of the system shown in Figure 7 (a) at 7.18 Hz: (a) time trace; (b) close up of (a); (c) probability density function (PDF); (d) autocorrelation

Table 4: Maximum RMS voltage obtained and bandwidth for each configuration for both the transverse and parametric directions

Configuration	Transverse Beam		Parametric Beam	
	Maximum RMS Voltage [V]	Bandwidth [Hz]	Maximum RMS Voltage [V]	Bandwidth [Hz]
A <sub>1</sub>	0.511	0.546	2.80	4.10
A <sub>2</sub>	4.72	1.97	3.92	4.24
B <sub>1</sub>	3.36	2.95	5.72	1.95
B <sub>2</sub>	6.59	2.08	5.72	2.35
C	6.60	2.29	5.67	1.14
D	5.63	1.72	4.94	1.46
E	6.05	1.53	4.30	0.632
F	6.54	0.953	3.20	0.271
No Stoppers	3.94	0.879	2.05	0.166

### Theoretical Comparisons

In this section, theoretical results have been compared to the experimentally obtained results to verify the model for the coupled parametric and transversely excited energy harvester.

COMSOL Multiphysics 5.1 has been used for the theoretical simulations; a non-dimensional motion amplitude has been introduced as the displacement divided by the thickness of the beam

(Displacement/h)—similarly, a non-dimensional excitation frequency has been derived as the excitation frequency divided by the fundamental frequency of the transverse and parametric beams,  $(\Omega/\omega_1)$ . The theoretically obtained fundamental frequencies of the transverse and parametrically excited beams were 6.924 and 4.607 Hz, respectively; this was within good agreement of the experimental results where were obtained to be 7.000 and 4.955 Hz, respectively. A comparison between the theoretical and experimental frequency-response curves for the transversely excited cantilever beam is shown in Figure 9; the theoretical and experimental results are within very good agreement of each other. Some discrepancy was observed between the theoretical and experimental comparisons between  $\Omega/\omega_1 = 0.85$  to 0.95 and  $\Omega/\omega_1 = 1.05$  to 1.15 which was due to the large amplitude motion resulting from the nonlinear curvature; however, when the system was moving greater than 10 mm, an excellent match between experiments and theory was obtained—discrepancies were also due to the complex behaviour of the piezoelectric bi-morph layer.

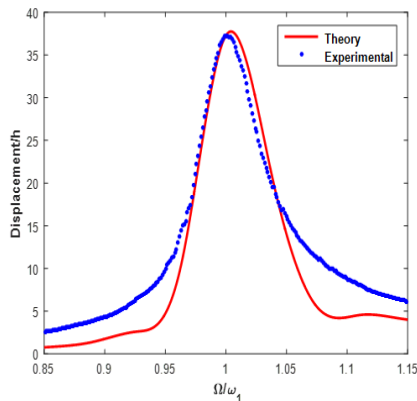


Figure 9: Theoretical and experimental comparison of non-dimensional frequency-response curves for the system ( $T_b$ ) with an excitation of  $1.5\text{m/s}^2$ .

## Conclusions

An energy harvesting device has been designed and fabricated based on the coupled excitation of a transverse and parametric cantilever-beams with mechanical stoppers; this design was selected to increase the nonlinear energy harvesting of the system and hence further enhance the effective operating

bandwidth at which the device can harvest energy—piezoelectric patches were selected as the energy transduction method. An electrodynamic shaker has been used to excite the L shaped energy harvester for various excitations and with various stopper configurations to investigate the added benefits of this unique design in further extending the operating bandwidth of the device.

With no stoppers, the transversely excited beam displayed a linear voltage; however, the parametric beam displayed a weak softening voltage-behaviour with period-doubling and saddle-node bifurcations. With dual-stopper configurations frequency-voltage curves of both the transverse and parametric core elements displayed a strong hardening-type nonlinear behaviour with the nonlinear frequency-voltage curves leaning towards the right; moreover, with single-stopper configurations, a hardening behaviour was also observed for both the systems; it was observed that the system could harvest energy over significantly larger bandwidth compared to the no stopper and one-stopper configurations; furthermore, as energy was extracted at higher frequencies, the RMS voltage was larger than the optimal one stopper configuration. For the theoretical investigation, the experimentally obtained fundamental and parametric frequencies and frequency-response curves are within good agreement. It can be concluded that the effect of coupling transversely and parametrically excited core elements in conjunction with mechanical stoppers further enhanced the nonlinear energy harvested over a much larger frequency-bandwidth (with the increase of 163.5%), hence proving the efficiency of the proposed device.

## References

- [1] Y. Ghiassi-Farrokhfal, S. Keshav, C. Rosenberg, and F. Ciucu, "Solar power shaping: an analytical approach," *IEEE Transactions on Sustainable Energy*, vol. 6, pp. 162-170, 2015.
- [2] Z. Tianpei and S. Wei, "Optimization of battery-supercapacitor hybrid energy storage station in wind/solar generation system," *IEEE Transactions on Sustainable Energy*, vol. 5, pp. 408-415, 2014.

- [3] J. Alejandro Franco, J. Carlos Jauregui, and M. Toledano-Ayala, "Optimizing wind turbine efficiency by deformable structures in smart blades," *ASME Journal of Energy Resources Technology*, vol. 137, pp. 051206-051206, 2015.
- [4] K. V. Wong and N. Tan, "Feasibility of using more geothermal energy to generate electricity," *ASME Journal of Energy Resources Technology*, vol. 137, pp. 041201-041201, 2015.
- [5] N. R. Tummuru, M. K. Mishra, and S. Srinivas, "Dynamic energy management of hybrid energy storage system with high-gain PV converter," *IEEE Transactions on Energy Conversion*, vol. 30, pp. 150-160, 2015.
- [6] W. Yu and D. Zhi-Quan, "Analysis of electromagnetic performance and control schemes of electrical excitation flux-switching machine for DC power systems," *IEEE Transactions on Energy Conversion*, vol. 27, pp. 844-855, 2012.
- [7] E. R. Westby and E. Halvorsen, "Design and modeling of a patterned-electret-based energy harvester for tire pressure monitoring systems," *IEEE/ASME Transactions on Mechatronics*, vol. 17, pp. 995-1005, 2012.
- [8] E. O. Torres and G. A. Rincon-Mora, "Electrostatic energy-harvesting and battery-charging CMOS system prototype," *IEEE Transactions on Circuits and Systems I: Regular Papers*, vol. 56, pp. 1938-1948, 2009.
- [9] X. Mininger, E. Lefeuvre, M. Gabsi, C. Richard, and D. Guyomar, "Semiactive and active piezoelectric vibration controls for switched reluctance machine," *IEEE Transactions on Energy Conversion*, vol. 23, pp. 78-85, 2008.
- [10] E. S. Leland and P. K. Wright, "Resonance tuning of piezoelectric vibration energy scavenging generators using compressive axial preload," *Smart Materials and Structures*, vol. 15, 2006/10/01/ 2006.
- [11] H. Yu, J. Zhou, X. Yi, H. Wu, and W. Wang, "A hybrid micro vibration energy harvester with power management circuit," *Microelectronic Engineering*, vol. 131, pp. 36-42, 2015/01/05/ 2015.
- [12] S. M. Shahruz, "Design of mechanical band-pass filters with large frequency bands for energy scavenging," *Mechatronics*, vol. 16, pp. 523-531, 2006/11// 2006.
- [13] V. R. Challa, M. G. Prasad, Y. Shi, and F. T. Fisher, "A vibration energy harvesting device with bidirectional resonance frequency tunability," *Smart Materials and Structures*, vol. 17, 2008/02/01/ 2008.
- [14] S. Leadenham and A. Erturk, "M-shaped asymmetric nonlinear oscillator for broadband vibration energy harvesting: Harmonic balance analysis and experimental validation," *Journal of Sound and Vibration*, vol. 333, pp. 6209-6223, 2014/11/24/ 2014.
- [15] B. P. Mann and N. D. Sims, "Energy harvesting from the nonlinear oscillations of magnetic levitation," *Journal of Sound and Vibration*, vol. 319, pp. 515-530, 2009/01/09/ 2009.
- [16] M. F. Daqaq, C. Stabler, Y. Qaroush, and T. Seuaciuc-Osório, "Investigation of power harvesting via parametric excitations," *Journal of Intelligent Material Systems and Structures*, vol. 20, pp. 545-557, March 1, 2009 2009.
- [17] L.-Q. Chen and W.-A. Jiang, "Internal resonance energy harvesting," *Journal of Applied Mechanics*, vol. 82, pp. 031004-031004, 2015.
- [18] Y. Wu, A. Badel, F. Formosa, W. Liu, and A. Agbossou, "Nonlinear vibration energy harvesting device integrating mechanical stoppers used as synchronous mechanical switches," *Journal of Intelligent Material Systems and Structures*, vol. 25, pp. 1658-1663, 2014/09/01/ 2014.